Dynamic braking of omni-wheel rollers for dual robot cooperative task execution
-Evaluation of magnetic gear based design for roller braking system-

Luis CANETE, Fukushima University ○,
luis@rb.sss.fukushima-u.ac.jp,
Takayuki TAKAHASHI, Fukushima University

This paper presents a novel wheel that features dynamic braking of the rollers of an omni-wheel. This results in interesting motions that would not be attained by ordinary wheels or the typical omni-wheel especially for dual differential drive robots. The design and prototype of the wheel is presented together with basic modeling.

Key Words : Omni-wheel, Cooperative Motion, Differential Drive

1. Introduction

The differential drive is commonly chosen for typical mobile robots due to its simple structure, relatively straightforward control and applicability to a wide array of environments. Differential drive systems require only two actuated wheels fixed in parallel on the mobile platform to achieve motion in a two dimensional plane including rotation. The maneuverability of the robot is sufficient for motion that a single robot performs.

The authors have been developing the Inverted Pendulum Type Assistant Robot (I-PENTAR) which employs the differential drive system. The I-PENTAR (Fig.1a) is able to use its own weight and balance to apply large forces which allows the application of a lightweight and low torque arm resulting in a relatively safe and functional assistant robot. This feature of the I-PENTAR has been studied, implemented and presented in [3][4] where the robot lifted a load and pushed a cart 20% and 45% its own weight respectively. This feature is unique and necessary for assistant robots that physically interact with humans.

Recently, the authors have been extending the capabilities of the I-PENTAR to include cooperative behavior with other robots or humans. These behaviors include cooperative lifting, pushing or pulling of objects and maybe even acting as a robotic walker and many more. In [2], it was shown that one of the difficulties of using the I-PENTAR for the cooperative tasks, especially for moving an objects, lies in the sliding constraints of the differential drive. Through kinematic modeling it was determined that some cooperative configurations result in poor maneuverability and even immobilization of the cooperative system. As a possible solution, a novel Switchable Omnidirectional Wheel (SOW) was proposed and prototyped by the authors and is shown in Fig.1b. The SOW can switch between omni-wheel and plain-wheel modes by engaging brake spokes on the rollers of an omni-wheel. This enables the I-PENTAR to function as a differential drive system with plain wheels when performing tasks as a single robot and then switch to omni-wheels to become a subsystem of an omnidirectional cooperative system. In [1] two differential drive mobile robots that implemented the SOW were developed by the authors and used to verify the kinematics and effectiveness of the SOW in cooperative tasks.

A special configuration for dual differential drive cooperative systems during object transportation exists when the wheels of the robots are inline while they face each other (Fig.1c). This is a configuration that limits robots with plain wheels to a single straight line path. Using the SOW and setting them to omni-wheel mode enables controllable translation along the y_B-axis and rotation along the origin. However,

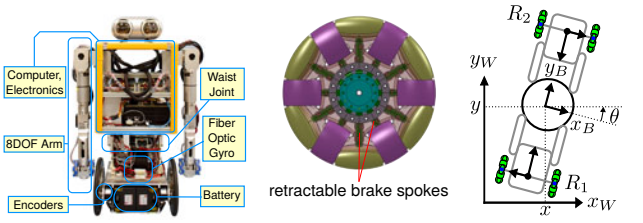

(a) I-PENTAR (b) SOW (c) Dual robot case

Fig.1 I-PENTAR and cooperative dual robot configuration

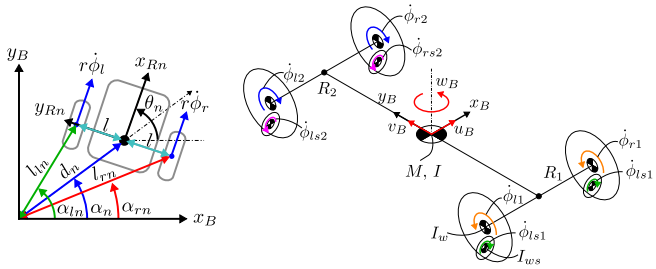

(a) Kinematic parameters (b) Dynamic parameters

Fig.2 Model parameters

motion along the x_B-axis becomes passive and uncontrollable limiting this configuration to flat surface and very low speeds. As an attempt to remedy this, the dynamic braking feature of the SOW is proposed. Instead of a hard switch between plain and omni-wheel modes, variable braking of the rollers is applied. This will generate a resistive forces in the direction of x_B-axis allowing passive control to be performed. To better understand the implication of using dynamic braking, the equations of motion specific to the aforementioned configuration is developed and a prototype of the mechanism capable of transmitting torque to the rollers is presented.

2. Kinematics for the dual robot case

It is important that the kinematics be introduced since they will be used during the derivation of the equations of motion. For an in-depth discussion of the kinematics for multi-robots using the SOW the reader is referred to [1].

First, the velocity vector of the object is assigned to be

Table 1 Model parameters

Symbol	Unit	Description
x,y	[m]	Pos. of object in x_W-y_W frame
θ	[rad]	Orient. of object in x_W-y_W frame
M	[kg]	Mass of entire system
I	[kgm^2]	Moment of Inertia of entire system
I_w	[m]	Moment of Inertia of wheel
I_{ws}	[m]	Moment of Inertia of rollers
r	[m]	Radius of wheel
r_s	[m]	Radius of rollers
τ_{r1},τ_{l1}	[Nm]	Input torque of R_1 wheels
τ_{rs1},τ_{ls1}	[Nm]	Input torque of R_1 rollers
τ_{r2},τ_{l2}	[Nm]	Input torque of R_2 wheels
τ_{rs2},τ_{ls2}	[Nm]	Input torque of R_2 rollers

$\boldsymbol{\nu}_B = [u_B,\, v_B,\, w_B]^T$. The location of each robot with respect to the object reference frame $x_B - y_B$ is defined by a distance d_n from the origin and an angle α_n measured from x_B. The orientation of the robot is θ_n (Fig.2a) and is measured form x_B. The kinematic model of the cooperative system is examined by determining the constraints of the left and right wheels of each robot. To simplify the development of the model, the parameters of each wheel is derived from the robot parameters d_n, α_n and θ_n.

$$l_{rn} = \sqrt{(d_n^2 + l^2 + 2d_n l \sin(\theta_n - \alpha_n)} \tag{1}$$

$$l_{ln} = \sqrt{(d_n^2 + l^2 - 2d_n l \sin(\theta_n - \alpha_n)} \tag{2}$$

$$\alpha_{rn} = \alpha_n - \tan^{-1}\left(\frac{l\cos(\theta_n - \alpha_n)}{d_n + l\sin(\theta_n - \alpha_n)}\right) \tag{3}$$

$$\alpha_{ln} = \alpha_n + \tan^{-1}\left(\frac{l\cos(\theta_n - \alpha_n)}{d_n - l\sin(\theta_n - \alpha_n)}\right). \tag{4}$$

The parameters for each wheel are applied to the equation below which assumes that that the wheels are all in omni-wheel mode.

$$\begin{bmatrix} \mathbf{J}_1 \\ \vdots \\ \mathbf{J}_n \\ \mathbf{J}_{s1} \\ \vdots \\ \mathbf{J}_{sn} \end{bmatrix} \boldsymbol{\nu}_B - \begin{bmatrix} r\dot{\boldsymbol{\phi}}_1 \\ \vdots \\ r\dot{\boldsymbol{\phi}}_n \\ r_s\dot{\boldsymbol{\phi}}_{s1} \\ \vdots \\ r_s\dot{\boldsymbol{\phi}}_{sn} \end{bmatrix} = \mathbf{0}, \tag{5}$$

where n is the number of robots,

$$\mathbf{J}_i = \begin{bmatrix} \cos\theta_i & \sin\theta_i & l_{ri}\sin\theta_i \\ \cos\theta_i & \sin\theta_i & l_{li}\sin\theta_i \end{bmatrix}, \dot{\boldsymbol{\phi}}_i = \begin{bmatrix} \dot{\phi}_{ri} \\ \dot{\phi}_{li} \end{bmatrix},$$

$$\dot{\boldsymbol{\phi}}_s i = \begin{bmatrix} \dot{\phi}_{rsi} \\ \dot{\phi}_{lsi} \end{bmatrix}, \mathbf{J}_{si} = \begin{bmatrix} \sin\theta_i & \cos\theta_i & -l_{ri}\cos\theta_i \\ \sin\theta_i & \cos\theta_i & -l_{li}\cos\theta_i \end{bmatrix},$$

and $i = 1..n$.

For the configuration shown in Fig.1c , $d_1 = 2l$, $\alpha_1 = -\frac{\pi}{2}$ and $\theta_1 = \frac{\pi}{2}$; $d_2 = 2l$, $\alpha_2 = \frac{\pi}{2}$ and $\theta_2 = -\frac{\pi}{2}$. Substituting these parameters into Eq.(5 the kinematic constraint is found to be

$$\begin{bmatrix} 0 & 1 & l_d \\ 0 & 1 & -l_d \\ 0 & -1 & l_d \\ 0 & -1 & -l_d \\ 1 & 0 & l_d \\ 1 & 0 & l_d \\ -1 & 0 & l_d \\ -1 & 0 & l_d \end{bmatrix} \boldsymbol{\nu}_B - r \begin{bmatrix} r\dot{\phi}_{r0} \\ r\dot{\phi}_{l0} \\ r\dot{\phi}_{r1} \\ r\dot{\phi}_{l1} \\ r_s\dot{\phi}_{rs0} \\ r_s\dot{\phi}_{ls0} \\ r_s\dot{\phi}_{rs1} \\ r_s\dot{\phi}_{ls1} \end{bmatrix} = \mathbf{0}, \tag{6}$$

where r is the radius of the wheels, r_s is the radius of rollers and $l_d = \sqrt{5l^2}$. In the actual wheel, the roller radius r_s varies depending on the contact point of the wheel with the ground but for simplicity it is assumed to be a constant value.

3. Modeling the dual robot system

To determine the effects of the applying dynamic braking on the rollers, the contribution of the individual wheels and rollers should be considered. Figure 2b shows the different rigid bodies and parameters involved in the model. Here, it is assumed that a single roller is in contact with the ground at all times. Furthermore, positive values of the input torques cause positive wheel and roller velocities.

To simplify model development the expressions for position will be omitted since there are no potential energy terms. The Lagrangian can then be directly determined to be

$$\begin{aligned} L =& \frac{1}{2}M\dot{x}^2 + \frac{1}{2}M\dot{y}^2 + \frac{1}{2}I\dot{\theta}^2 + \frac{1}{2}I_w\dot{\phi}_{r1} + \frac{1}{2}I_w\dot{\phi}_{l1} \\ &+ \frac{1}{2}I_w\dot{\phi}_{r2} + \frac{1}{2}I_w\dot{\phi}_{l2} + \frac{1}{2}I_{ws}\dot{\phi}_{rs1} + \frac{1}{2}I_{ws}\dot{\phi}_{ls1} \\ &+ \frac{1}{2}I_{ws}\dot{\phi}_{rs2} + \frac{1}{2}I_{ws}\dot{\phi}_{ls2}, \end{aligned} \tag{7}$$

which are clearly all kinetic energy terms. Using Lagrangian's equation and choosing the generalized coordinates to be

$$\mathbf{q} = [x,\, y,\, \theta,\, \phi_{r1},\, \phi_{l1},\, \phi_{r2},\, \phi_{l2},\, \phi_{rs1},\, \phi_{ls1},\, \phi_{rs2},\, \phi_{ls2}]^T$$

and the generalized forces

$$\boldsymbol{\tau} = [\tau_{r1},\, \tau_{l1},\, \tau_{r2},\, \tau_{l2},\, \tau_{rs1},\, \tau_{ls1},\, \tau_{rs2},\, \tau_{ls2}]^T$$

yields the differential equation

$$\mathbf{M}\ddot{\mathbf{q}} = \mathbf{E}\boldsymbol{\tau}, \tag{8}$$

where

$$\mathbf{M} = \mathrm{diag}\,(M,\, M,\, I,\, I_w,\, I_w,\, I_w,\, I_w,\, I_{ws},\, I_{ws},\, I_{ws},\, I_{ws}),$$

and

$$\mathbf{E} = \begin{bmatrix} \mathbf{0}_{(3\times 8)} \\ \mathbf{I}_{(8\times 8)} \end{bmatrix},$$

where $\mathbf{0}$ is a zero matrix and $\mathbf{I}$ is an identity matrix. The differential equation of Eq.(8) is incomplete because it does not take into consideration the kinematic constraints of Eq.(6). The constraints can be applied by choosing the velocity vector $\boldsymbol{\nu}_B = [u_B\, v_B\, w_B]^T$ to be the new state variables and establishing that

$$\dot{\mathbf{q}} = \mathbf{S}(\mathbf{q})\boldsymbol{\nu}_B \tag{9}$$

$$\ddot{\mathbf{q}} = \dot{\mathbf{S}}(\mathbf{q})\boldsymbol{\nu}_B + \mathbf{S}(\mathbf{q})\dot{\boldsymbol{\nu}}_B, \tag{10}$$

where

$$\mathbf{S}(\mathbf{q}) = \begin{bmatrix} \cos\theta & -\sin\theta & 0 \\ \sin\theta & \cos\theta & 0 \\ 0 & 0 & 1 \\ 0 & \frac{1}{r} & \frac{l_d}{r} \\ 0 & \frac{1}{r} & -\frac{l_d}{r} \\ 0 & -\frac{1}{r} & \frac{l_d}{r} \\ 0 & -\frac{1}{r} & -\frac{l_d}{r} \\ \frac{1}{r_s} & 0 & \frac{l_d}{r_s} \\ \frac{1}{r_s} & 0 & \frac{l_d}{r_s} \\ -\frac{1}{r_s} & 0 & \frac{l_d}{r_s} \\ -\frac{1}{r_s} & 0 & \frac{l_d}{r_s} \end{bmatrix}. \quad (11)$$

Note that the first three rows of $\mathbf{S}(\mathbf{q})$ is a rotation matrix that projects the vector $\boldsymbol{\nu}_B$ to $[\dot{x}, \dot{y}, \dot{\theta}]^T$ in the $x_W - y_W$ frame. The lower 8 rows are simply derived from the kinematic constraints of Eq.(6).

And so by substituting Eq.(9) and (10) into Eq.(8), the equations of motion can be updated and simplified to

$$\hat{\mathbf{M}}\dot{\boldsymbol{\nu}}_B + \hat{\mathbf{H}}\boldsymbol{\nu}_B = \hat{\mathbf{E}}\boldsymbol{\tau}, \quad (12)$$

where

$$\hat{\mathbf{M}} = \mathbf{S}^T\mathbf{M}\mathbf{S} \equiv \begin{bmatrix} \frac{4I_{ws}+Mr_s^2}{r_s^2} & 0 & 0 \\ 0 & \frac{4I_w+Mr^2}{r^2} & 0 \\ 0 & 0 & \frac{4I_{ws}l^2r^2+4I_wl^2r_s^2+r^2r_s^2I}{r^2r_s^2} \end{bmatrix},$$

$$\hat{\mathbf{H}} = \mathbf{S}^T\mathbf{M}\dot{\mathbf{S}} \equiv \begin{bmatrix} 0 & -Mw_B & 0 \\ Mw_B & 0 & 0 \\ 0 & 0 & 0 \end{bmatrix},$$

$$\hat{\mathbf{E}} = \mathbf{S}^T\mathbf{E} \equiv \begin{bmatrix} 0 & 0 & 0 & 0 & \frac{1}{r_s} & \frac{1}{r_s} & -\frac{1}{r_s} & -\frac{1}{r_s} \\ \frac{1}{r} & \frac{1}{r} & -\frac{1}{r} & -\frac{1}{r} & 0 & 0 & 0 & 0 \\ \frac{l_d}{r} & -\frac{l_d}{r} & \frac{l_d}{r} & -\frac{l_d}{r} & \frac{l_d}{r_s} & \frac{l_d}{r_s} & \frac{l_d}{r_s} & \frac{l_d}{r_s} \end{bmatrix}.$$

3.1 Effect of dynamic braking

Inspection of Eq.(12) shows that $\hat{\mathbf{M}}$ is a diagonal matrix and therefore its inverse is also diagonal. Using this information, the equation of motion along x_B can be extracted as

$$\dot{u}_B = \frac{r_s^2}{4I_{ws}+Mr_s^2}\left(Mw_Bv_B + \frac{1}{r_s}(\tau_{rs1}+\tau_{ls1}-\tau_{rs2}-\tau_{ls2})\right). \quad (13)$$

It can be seen that without the input torques of the rollers, controllable motion along u_B is difficult. Although the first term of Eq.(13) can be accessed by controlling v_B or w_B to generate some acceleration, the required velocity would be large and difficult to apply for the targeted cooperative system.

Dynamic braking of the rollers requires resistance to motion but not totally inhibit it. This resistance to motion can be applied through the input torques of the rollers. There are many possible ways of representing the resistive torques but for simplicity they are assigned to be

$$\tau_{rs1} = -K_{r1}\dot{\phi}_{rs1},\ \tau_{ls1} = -K_{l1}\dot{\phi}_{ls1}$$
$$\tau_{rs2} = -K_{r2}\dot{\phi}_{rs2},\ \tau_{ls2} = -K_{l2}\dot{\phi}_{ls2}, \quad (14)$$

where K_{r1}, K_{l1}, K_{r2} and K_{l2} are assumed to be variable and controllable but never negative.

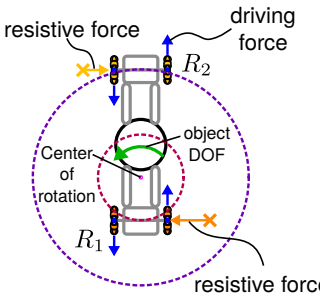

Fig.3 Possible motion with dynamic braking

Two components are required to generate a nonzero $\dot{u}_B$. The first is that the rollers must be rotating with nonzero velocities. From Eq.(12) it can be seen that the wheel input torques can influence the roller velocity through w_B. A trivial way of achieving this is by assigning the wheel input torques to be

$$\tau_{r1} = u, \tau_{l1} = -u \quad (15)$$
$$\tau_{r2} = u, \tau_{l2} = -u, \quad (16)$$

where u is an arbitrary value. The second component is that $K_{r1} + K_{l1}$ is not equal to $K_{r2} + K_{l2}$ which would cause a nonzero acceleration in $\dot{u}_B$. The motion that can be achieved is shown in Fig.3 where the instantaneous center of rotation is located not at the origin of the object but offset from it. The the offsett can be varied by changing the difference between $K_{r1} + K_{l1}$ and $K_{r2} + K_{l2}$. Clearly, this is an improvement compared to the lack of controllability in the x_B direction. In fact, by using small oscillatory rotations with synchronized dynamic braking, the system is able to move sideways along u_B. This is an important feature when transporting large objects in small spaces.

4. Wheel design and prototype

The original SOW only required the rollers to be locked or unlocked and so contact friction was the simplest yet effective method that could be used. By simultaneously pushing upon all the rollers using spokes, they could be locked in place enabling plane wheel mode. Minute variations in friction between different rollers did not cause problems since sufficient application of pressure could be performed to ensure braking. However, for dynamic braking variations in friction come into play making equal braking for all the rollers difficult. Furthermore, using contact friction as a braking method could possibly cause abrasion on the rollers which result in wear and tear.

Another solution involves the use of coils that would be embedded into the rollers. These coils would be shorted internally and moving a permanent magnet close would induce currents in the coil that would then cause a resistance to rotation. The closer the magnet the larger the resistance. The problem with this methodology is that the torque would be insufficient. In theory a speed reducer like a gear could be used to increase the torque but attaching this to every single roller on the wheel would not be practical.

On the other hand, if torque could be transmitted to all rollers from a single braking device then the design would be simplified significantly. As an initial step in this direction, the authors propose a magnetic transmission system for omni-wheel rollers. The transmission system is based on the MagTran [5]. In place of gear teeth, MagTran uses a series

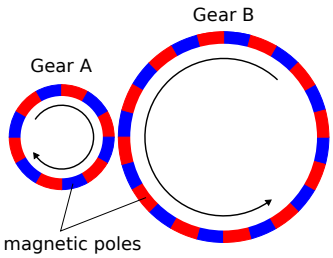

Fig.4 Magnet gear principle

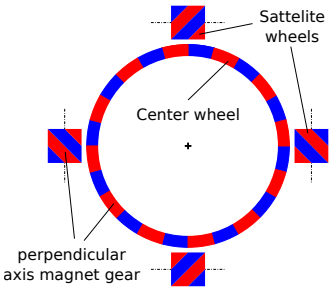

Fig.5 Driving multiple magnet gears

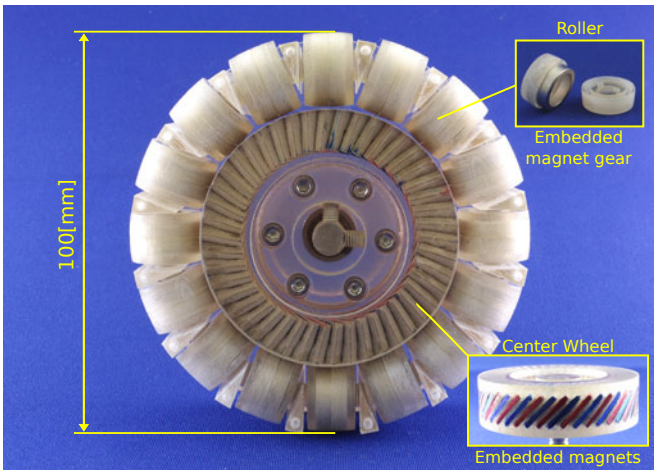

Fig.6 Omni-wheel with magnetic transmission system for rollers

of magnetic poles pairs arranged in a circle around a wheel (Fig.4). Since the magnetic force is strongest where the distance between the wheels is closest, turning one wheel would move that specific pole pair and transmit motion to the corresponding pole pair on the other wheel. There are mainly two types of gears, parallel axis gears and perpendicular axis gears. For the proposed magnetic transmission system, perpendicular axis gears are chosen so that a center wheel will drive the surrounding satellite wheels (Fig.5).

4.1 Prototype magnetic transmission system

The prototype of the magnetic transmission system for the omni-wheel is shown Fig.6. Unlike the original SOW, the authors have opted not to implement the omni-wheel design based on [6] to simplify the initial design. The prototype has a diameter of 100[mm] and has 16 rollers of identical size. Each roller is embedded with a FD-16-C magnet gear that has a diameter of 16[mm] and a maximum transmissible torque of 0.14[kgf·cm]. To reduce the air gap between the center wheel and the satellite wheels, the center wheel was chosen to be 63[mm]. However, since magnet gears with a diameter of 63[mm] from MagTran do not exist, the authors prototyped a magnet gear using rectangular neodymium magnets embedded into a 3D printed center wheel frame. In total, there are 46 rectangular magnets that are arranged so that the poles facing out towards the satellite wheels alternate. Since the magnet gear embedded in the rollers have 12 poles the gear ratio between the center wheel and rollers is 1:3.83. Initial testing of the prototype shows that the satellite wheels rotate smoothly without any unwanted contact between the center wheel and satellite wheels. There is significant torque but precise and accurate measurement have not yet been performed.

5. Conclusion

Analysis and testing of a dual robot cooperative system that uses the SOW showed that in configurations where the robots face each other sideways motion is not controllable. To remedy this, the dynamic braking feature was proposed and the modeling of the equations of motion showed that performance can be improved. Initial design of an omni-wheel with dynamic roller braking was undertaken by developing the transmission system for the rollers using magnetic gears. The magnetic transmission system was prototyped and showed that torque could be applied to all the rollers simultaneously. Future work will involve the application of a braking device to the proposed wheel to achieve dynamic braking. And perhaps, if the magnet gears can achieve sufficient holding torque the transmission system may be extended to actively actuating the rollers.

References

[1] L. Canete, T. Takahashi, Development of a novel Switchable Omnidirectional Wheel for performing cooperative tasks using differential drive mobile robots, Proceedings of the IEEE/RSJ International Conference on Intelligent Robots and Systems, Vancouver, Canada, 2017,pp. 6979-6984.

[2] L. Canete, T. Takahashi, Development of a novel omnidirectional wheel for differential drive mobile robots -Basic kinematic modeling and prototype development-, Proceedings of the JSME Conference on Robotics and Mechatronics, Yokohama, Japan, 2016, 2A2-07b7.

[3] L. Canete, T. Takahashi, Modeling, Analysis and Compensation of Disturbances During Task Execution of A Wheeled Inverted Pendulum Assistant Robot Using a Unified Controller, Advanced Robotics Vol. 29, Iss. 22, pp.1453-1462, 2015.

[4] L. Canete, T. Takahashi, A Disturbance Compensation Method for Pushing Control of an Inverted Pendulum Robot, Proceedings of the 29th Annual Conference of the Robotics Society of Japan, Tokyo, Japan, 2011, 1I3-8.

[5] “MagTran: A toothless gear system (translated from japanese),”.[Online]. Available: http://www.magtran.com/. Accessed: March 6,2018.

[6] 淺間一,嘉 早人,遠藤,佐藤雅俊:“全方向移動車用車輪”,3421290,4553.